

Published in final edited form as:

J Gene Med. 2012 February ; 14(2): 77–89. doi:10.1002/jgm.1649.

EphrinA1-EphA2 interaction-mediated apoptosis and Flt3L-induced immunotherapy inhibits tumor growth in a breast cancer mouse model

Manish Tandon, Sai V. Vemula, Anurag Sharma, Yadvinder S. Ahi, Shalini Mittal, Dinesh S. Bangari¹, and Suresh K. Mittal*

Department of Comparative Pathobiology, Purdue University Center for Cancer Research, and Bindley Bioscience Center, Purdue University, West Lafayette, IN

Abstract

Background—The receptor tyrosine kinase EphA2 is overexpressed in several types of cancers and is currently being pursued as a target for breast cancer therapeutics. The EphA2 ligand EphrinA1 induces EphA2 phosphorylation and intracellular internalization and degradation, thus inhibiting tumor progression. The hematopoietic growth factor, FMS-like tyrosine kinase receptor ligand (Flt3L), promotes expansion and mobilization of functional dendritic cells.

Methods—We tested the EphrinA1-EphA2 interaction in MDA-MB-231 breast cancer cells focusing on the receptor-ligand-mediated apoptosis of breast cancer cells. In order to determine whether the EphrinA1-EphA2 interaction-associated apoptosis and Flt3L-mediated immunotherapy would have an additive effect in inhibiting tumor growth, we used an immunocompetent mouse model of breast cancer to evaluate intratumoral (i.t.) inoculation strategies with human adenovirus (HAd) vectors expressing either EphrinA1 (HAd-EphrinA1-Fc), Flt3L (HAd-Flt3L) or a combination of EphrinA1-Fc + Flt3L (HAd-EphrinA1-Fc + HAd-Flt3L).

Results—*In vitro* analysis demonstrated that an EphrinA1-EphA2 interaction led to apoptosis-related changes in breast cancer cells. *In vivo*, three i.t. inoculations of HAd-EphrinA1-Fc showed potent inhibition of tumor growth. Furthermore, increased inhibition in tumor growth was observed with the combination of HAd-EphrinA1-Fc and HAd-Flt3L accompanied by the generation of an anti-tumor adaptive immune response.

Conclusions—The results indicating induction of apoptosis and inhibition of mammary tumor growth show the potential therapeutic benefits of HAd-EphrinA1-Fc. In combination with HAd-Flt3L, this represents a promising strategy to effectively induce mammary tumor regression by HAd vector-based therapy.

Keywords

EphA2; EphrinA1; Flt3L; immunotherapy; breast cancer; adenovirus vector

*Corresponding author: Suresh K. Mittal, Department of Comparative Pathobiology, School of Veterinary Medicine, Purdue University, West Lafayette, IN 47907, USA, Tel: (001) 765-496-2894, Fax: (001) 765-494-9830, mittal@purdue.edu.

¹Current address: Department of Pathology, Genzyme Corporation, 5 Mountain Road, Framingham, MA

CONFLICT OF INTEREST STATEMENT

The authors declare no conflict of interest.

INTRODUCTION

The heterogeneous and infiltrative nature of breast cancers, their potential for distal metastasis and development of drug resistance are key elements responsible for the reduced efficacy of current therapeutic approaches [1,2]. In addition, a dysfunction in apoptosis or programmed cell death resulting in over-proliferation and survival of cells is a principle problem in anti-cancer therapeutics [3,4]. A complex network of molecular signaling regulates apoptosis mainly through death receptor (extrinsic) or mitochondrial (intrinsic) pathways. These de-regulated apoptotic mechanisms in cancer cells are also responsible, in part, for the development of resistance towards anti-cancer cytotoxic agents [5-7]. The selective induction of apoptosis in cancer cells and the correction of aberrant apoptotic signaling pathways is a promising strategy for cancer drug discovery [8]. Therefore, novel approaches are needed to simultaneously target cancer cells, prevent distal metastasis and induce long lasting anti-cancer immunity.

The EphA2 receptor tyrosine kinase is overexpressed in multiple cancers and is correlated to poor prognosis in advanced cancer cases; therefore, it is regarded as a fine target for therapeutic intervention [9-11]. Lower levels of EphA2 protein have been detected in non-tumorigenic mammary epithelial cells (e.g., MCF-10A) and clinical specimens of benign mammary epithelium compared to the elevated expression of EphA2 observed in transformed and aggressive mammary epithelial cells (e.g., MDA-MB-231), and clinical specimens of breast carcinoma [12]. This EphA2 overexpression had been related to mammary tumorigenesis and the development of a malignant phenotype. Pre-clinical targeting of EphA2 overexpression via agonist antibodies and cytotoxic therapies has generated beneficial anti-tumor responses [13-16]. In addition, reducing EphA2 expression has enhanced sensitivity to the human epidermal growth factor receptor 2 (Her2)-targeted monoclonal antibody therapy in pre-clinical breast cancer models [17,18]. EphA2-derived peptide epitopes have activated CD4⁺ and CD8⁺ T cell responses against EphA2 [19]. Combinations of the EphA2 ligand, EphrinA1, or EphA2 agonist antibodies supplemented with anti-EphA2 CD8⁺ T cells completely eliminated renal carcinoma-induced tumors in a mice model [20]. All these results indicate that targeting EphA2 overexpression via a combination of approaches may provide better therapeutic efficacy for breast cancer treatment.

Additionally, the expression of a secretory-form of EphrinA1 by an adenovirus (Ad) vector (HAd-EphrinA1-Fc) in EphA2 overexpressing mouse mammary tumor-derived MT1A2 cells induced EphA2 phosphorylation resulting in a decrease of EphA2 expression and cell viability [21]. In an immunocompetent mouse model, not only did inoculation of HAd-EphrinA1-Fc-infected MT1A2 cells prevent the formation of tumors, but a single intratumoral (i.t.) injection of HAd-EphrinA1-Fc also delayed tumor growth on existing tumors [22]. The incomplete tumor regression may be due to the failure of HAd-EphrinA1-Fc or the expressed EphrinA1 to reach a large number of cells in the tumor mass.

FMS-like tyrosine kinase 3 ligand (Flt3L) is a ligand for the tyrosine kinase receptor Flt3 and regulates the differentiation of hematopoietic progenitor cells [23,24]. The Flt3 and

Flt3L-mediated signaling pathway regulates the generation and differentiation of plasmacytoid, resident and migratory dendritic cells (DC) from bone marrow progenitor cells [25,26]. The EphA2 transcript, in addition to its expression in epithelial cells, is also present in immune tissues such as the spleen, bone marrow and lymph nodes [27]. There is also evidence of expression of EphA2 in both DC cultured *in vitro* and in Langerhans cells residing in epidermis, fostering the idea that EphA2 could function in DC trafficking and localization [28]. The stimulation of DC with Flt3L promotes their clonal expansion in the spleen, bone marrow, lymph nodes and peripheral blood. The DC are potent antigen presenting cells (APC) that function in the context of a major histocompatibility complex (MHC) and co-stimulatory molecules to effectively stimulate specific immune responses. The Flt3L markedly enhances the DC function, elevates the natural killer (NK) cells number, and induces both tumor regression and anti-tumor immune responses [29-31]. In melanoma and renal cancer patients, Flt3L administration has resulted in an increase in the CD11c⁺ DC population [32]. Transgenic mice lacking Flt3L show reduced bone marrow progenitor cells, NK cells, and myeloid- and lymphoid-related DC [23]. Notably, the infiltration of DC and CD8⁺ T cells in the tumor tissue correlates to a favorable prognosis, while macrophage infiltration may represent a poor prognosis [33,34]. Given the central role of DC as APC in the immune system, these findings indicate that stimulation with Flt3L might enhance the immune response to breast cancer.

The administration of Flt3L in combination with local radiotherapy reduced pulmonary metastasis and enhanced survival in a mouse model of metastatic lung cancer [35,36]. Additionally, in murine models of breast cancer, colon cancer, melanoma and sarcoma, a recombinant Flt3L protein or an expression plasmid carrying Flt3L cDNA resulted in anti-tumor effects when administered alone or in combination with other therapies [31,37,38]. Ad vector-mediated Flt3L in combination with radiation therapy or chemotherapy has been shown to have beneficial effects on tumor regression and the development of an immunologic memory [39-44]. Despite evidence that both EphA2 and Flt3 receptor-targeted approaches have resulted in preclinical anti-cancer effects, EphA2 functions mainly via cytotoxic mechanisms while Flt3 functions by immunologic mechanisms. We reason that the EphrinA1-mediated killing of EphA2 overexpressing MT1A2 cells will generate tumor-associated antigens and that, if presented to Flt3L-mobilized APC in the tumor microenvironment will result in an anti-tumor immune response. A combination of EphA2 and Flt3-targeted therapies would thus result in better and long-lasting anti-cancer response. In this study, we investigated whether the therapeutic efficacy of Ad-mediated EphrinA1 expression in mammary cancers could be enhanced by multiple i.t. inoculations both alone or in combination with Flt3L immunotherapy in an immunocompetent mouse model of breast cancer. Our results indicate that EphrinA1-EphA2 interaction induces cancer cell-specific apoptosis and enhances the inhibition of tumor growth when used in combination with Flt3L immunotherapy.

MATERIALS AND METHODS

Cell lines and Ad vectors

The bovine-human hybrid (BHH-2C) [45], human embryonic kidney (HEK 293), human mammary epithelium (MCF-10A), transformed human mammary (MDA-MB-231) and transformed mouse mammary (MT1A2) [46] cell lines were propagated as previously described [21]. The MT1A2 cell line was kindly provided by Dr. William Muller, Department of Biology, McMaster University, Hamilton, Ontario, Canada. The construction of a replication defective HAd5 vector (HAd-EphrinA1-Fc) with deletions in the E1 and E3 regions and containing EphrinA1-Fc in the E1 region has been previously described [21]. The secretory-form of the Flt3L gene derived from the PubMed nucleotide database (Accession: NM_001459) was commercially (*Genscript Inc.*, Piscataway, NJ, USA) synthesized. The Flt3L gene under the control of a CMV promoter was cloned into the shuttle plasmid pDC311 (*Microbix, Inc.*, Toronto, Ontario, Canada) to generate pDC311-Flt3L. To construct the HAd vector expressing Flt3L (HAd-Flt3L), pDC311-Flt3L was co-transfected with a HAd genomic plasmid lacking the E1 and E3 regions (pBHGlox E1,3Cre) in the 293Cre cell line (a gift from Merck, Inc., Whitehouse Station, NJ) [47] by calcium phosphate-mediated transfection. The vectors, HAd-EphrinA1-Fc, HAd-Flt3L and the empty vector (HAd- E1E3), were propagated in the HEK 293 cell line and purified by cesium chloride-density gradient centrifugation as previously described [48]. The purified virus preparation was titrated by plaque formation assay in the BHH-2C cell line. The EphrinA1 and Flt3L protein expression was confirmed by Western blot analyses.

Real-time PCR

MDA-MB-231 cells were mock-infected or infected with 100 plaque-forming units (pfu)/cell of HAd- E1E3 or HAd-EphrinA1-Fc, and the total cellular RNA was isolated using a column-based RNA isolation kit (*Stratagene Inc.*, La Jolla, CA, USA) following the manufacturer's instructions. A designed array of PCR primers (96-well format) for a panel of genes implicated in carcinogenesis along with housekeeping genes was obtained commercially [Human Cancer Pathway Finder PCR Array (PAHS-033A), *SABiosciences*, Frederick, MD, USA]. The array included representative genes for the cell cycle control, DNA damage repair, apoptosis, cell adhesion, invasion, metastasis and angiogenesis. The real-time quantitative PCR with SYBR chemistry and relative gene expression data analysis was performed according to manufacturer's instructions (*Stratagene Inc.*). The gene expression levels were normalized with three internal control genes (β -Actin, GAPDH and RPL13A). The fold changes in gene expression for HAd-EphrinA1-Fc treated cells were calculated with respect to HAd- E1E3 control vector treated cells.

Apoptosis assays

Nuclear morphology—MCF-10A, MDA-MB-231, or MT1A2 cells (5000 cells/well) were seeded overnight in a chamber slide. The next day the cells were either mock-infected or infected with 100 pfu/cell of HAd- E1E3 or HAd-EphrinA1-Fc and incubated for 48 h at 37°C in a CO₂ incubator. The cells were then washed once in phosphate-buffered saline (PBS), fixed with 4% paraformaldehyde and permeabilized with 1% Triton X-100 in PBS. The cells were then stained with the DAPI (4, 6-diamino-2-phenylindole) nuclear stain and

photographed under a fluorescence microscope. The number of normal nuclei per field in six representative images was enumerated.

Annexin V staining—MCF-10A, MDA-MB-231, or MT1A2 cells were either mock-infected or infected with 100 pfu/cell of HAd- E1E3 or HAd-EphrinA1Fc. At 48 h post-infection the adherent cells were harvested by trypsinization, incubated with Annexin V-FITC and propidium iodide (PI) and then analyzed by flow cytometry. An Annexin V-FITC apoptosis detection kit (Catalog number 556547, *BD Biosciences*, San Jose, CA, USA) was utilized for this assay following the manufacturer's instructions.

Western blot analysis

MCF-10A, MDA-MB-231, or MT1A2 cells were mock-infected or infected with 100 pfu/cell of HAd- E1E3 or HAd-EphrinA1-Fc. At 24 and 48 h post-infection, cells were harvested, and whole cell lysates were prepared for SDS-PAGE followed by Western blot analyses as previously described [21]. The blots were probed with antibodies specific for maspin, TNF, Bcl2, Bad, Bok, Bax, Bmf, Puma, caspase-3 (full length and cleaved), caspase 7 (full length and cleaved), PARP (*Cell Signaling*, Danvers, MA, USA), and p-21 (*Santa Cruz Biotechnology*, Santa Cruz, CA, USA) proteins. All blots, after stripping, were probed with anti- β -Actin antibody (*Sigma Aldrich Corp.*, St. Louis, Mo, USA) to verify equal loading.

Animal inoculation study

Six to eight week-old female FVB/n mice were obtained from Harlan Laboratories (Indianapolis, IN, USA), and the experiments were performed as per the guidelines of the Institutional Biosafety Committee and Institutional Animal Care and Use Committee. Animals were inoculated subcutaneously (s.c.) into the right axillary region with 0.5×10^6 MT1A2 cells suspended in serum-free and antibiotic-free Eagle's minimum essential medium. The tumor-bearing mice were randomly divided (32 mice per group) into following groups: control (PBS), HAd- E1E3 (10^9 pfu/mice), HAd-EphrinA1-Fc (10^9 pfu/mice), HAd-Flt3L (10^8 pfu/mice) and HAd-EphrinA1-Fc+HAd-Flt3L (10^9+10^8 pfu/mice). The study was divided into two stages.

For Stage I, vector inoculations were initiated one week post MT1A2 cell inoculation when the tumors were not palpable. The site of MT1A2 cell inoculation had been marked to enable vector inoculation at the same site. These groups were further divided into subgroups (8 mice per group) receiving one dose (on Day 7) or three doses (on Days 7, 10, and 13) of vector inoculations. For Stage II, i.t. vector inoculations were initiated when palpable tumors were present (30-50 mm³ in size). The palpable tumors developed at approximately two weeks post MT1A2 inoculation. Similar to Stage I, the Stage II groups were further divided into subgroups (8 mice per group) receiving one or three doses (three days apart) of vector inoculations. The tumor growth was monitored weekly by Vernier Caliper readings. The tumor volume was calculated using the formula [$\text{length} \times (\text{width}^2)/2$] as previously described [22].

Immunohistochemistry

The tumors' tissues were embedded in O.C.T. (Optimal Cutting Temperature) compound in plastic molds, frozen in liquid nitrogen and stored at -80°C until sectioning. Cryosections, 4-5µm in thickness, were cut at Purdue University's Histology and Phenotyping Laboratory. The sections were fixed in acetone and air dried. They were then incubated with an antibody specific to the cleaved caspase 3 or cleaved PARP (*Cell Signaling*), CD11c and CD8 (*Biolegend Inc.*, San Diego, CA). The immunohistochemical staining was performed as previously described [48].

ELISpot and Cytotoxicity assays

The Stage II mouse groups that had been inoculated three times with Ad vectors were euthanized on Day 45, and the spleens were aseptically removed. Naïve mice without tumors served as untreated negative controls. An ELISpot assay was performed following a previously described protocol with some modifications [49]. To utilize tumor-specific antigens arising as a result of cell apoptosis and death as opposed to only cell surface antigens, the total MT1A2 cell lysate was prepared by disrupting the cells with three freeze-thaw cycles; this lysate was used to stimulate the splenocytes [50]. For the cytotoxicity assays, the total splenocytes were co-cultured with mitomycin-treated (10µg/ml mitomycin) MT1A2 cells for five days in RPMI medium supplemented with 50 units/ml of recombinant mouse IL-2 (*eBiosciences*, San Diego, CA, USA). CD8+ T cells were enriched from the total splenocyte population using mouse CD8a (Ly-2) micro-beads in a magnetic cell sorting apparatus as per the manufacturer's instructions (*Miltenyi Biotec*, Auburn, CA, USA). A quantitative determination of CD8+ cell-induced cytotoxicity was carried out by a colorimetric lactate dehydrogenase (LDH) cytotoxicity assay (*Promega Inc.*, Madison, WI, USA). CD8+ cells from naïve mice or mice i.t. inoculated with PBS, HAd- E1E3, HAd-EphrinA1-Fc, HAdFlt3L or a combination of HAd-EphrinA1-Fc + HAdFlt3L were co-incubated in triplicates with 10,000 MT1A2 cells in a 96-well culture dish in 1:1 ratio. The LDH released into the supernatant was detected by measuring absorbance at 490nm with a spectrophotometer. The absorbance from treated cells was corrected for background absorbance from media, CD8 cells or MT1A2 cells to determine percent cytotoxicity.

Statistical analysis

Data were presented as mean ± standard deviation. The *P* values to test the significance within groups were derived from unpaired student's t-test for a two treatment comparison or with the ANOVA procedure with Tukey's adjustments for more than two treatment comparisons. A *P* value of less than 0.1 and 0.05 was considered as marginally and statistically significant, respectively.

RESULTS

EphrinA1-Fc expression in mammary cancer cells induces apoptosis-related phenotypic alterations

We had earlier demonstrated that expression of the secretory-form of EphrinA1 by HAd-EphrinA1-Fc resulted in enhanced EphA2 phosphorylation and its turnover [21,22]. This

was positively correlated to growth inhibition and induction of cytotoxicity in MDA-MB-231 and MT1A2 cancer cells (Supplementary Fig. 1a-c). To further investigate the potential mechanism/s of EphrinA1-EphA2 interaction-mediated apoptosis-related changes, *in vitro* phenotypic analysis of HAd-EphrinA1-Fc-infected MDA-MB-231 and MT1A2 cells was performed. The analysis showed that a high percentage of cells had condensed and fragmented nuclei in the HAd-EphrinA1-Fc-infected MDA-MB-231 or MT1A2 cells (Fig. 1a). The nuclear condensation, deformation and fragmentation were more pronounced in MT1A2 cells compared to MDA-MB-231 cells, while MCF-10A cells were largely unaffected (Fig. 1b). In order to determine if the alterations in nuclear morphology were due to apoptotic changes, HAd-EphrinA1-Fc-infected cells were stained with AnnexinV-FITC and propidium iodide (PI), analyzed by flow cytometry, and then compared with a HAd-E1E3 empty vector. There was a more than three-fold increase in the percentage of MDA-MB-231 and MT1A2 cells stained with AnnexinV and PI suggesting the enhancement of apoptosis following infection with HAd-EphrinA1-Fc. (Fig. 1c).

EphrinA1-Fc expression modulates apoptosis-related gene expression and post-translational regulatory mechanisms

To further investigate the EphrinA1-Fc-EphA2 interaction-mediated changes in cancer cells, MDA-MB-231 cells were infected with HAd-EphrinA1-Fc or HAd-E1E3, and the total cellular RNA was isolated at 24 and 48 h post-infection. RNA samples were used to monitor the alterations in gene expression of a panel of cancer-related genes in a gene array by RT-PCR assay. Expression levels of β -Actin, GAPDH and RPL13A served as internal controls. The most prominent alterations of EphrinA1-Fc expression in MDA-MB-231 cells were the two to three-fold increase in the gene expression of p-21 (CDKN1A), IL8, Maspin (Serpina5), TEK/Tie2, Itga4, MMP1 and TNF α compared to the empty vector (HAd-E1E3) control (Figure 2a and Supplementary Table 1). Expression levels of other cancer- or apoptosis-related genes including Bcl-2 family showed little or no change either at 24 or 48 h.

To determine whether the changes in gene expression levels correlated with protein expression, HAd-EphrinA1-Fc-infected MDA-MB-231 or MT1A2 cells were analyzed for expression levels of the Bcl-2 family proteins, p21, maspin, and TNF α by Western blot analyses. In MDA-MB-231 cells, a 30% decline in pro-survival Bcl-2 and Bcl2-xL and a 40% increase in pro-apoptotic Bad protein expression were evident at 24 h post infection (Fig. 2b). In MT1A2 cells, the Bcl-2 protein expression also declined, while the Bcl2-xL (30% increase) and Bad (50% reduction) proteins showed the reverse of the protein expression levels in MDA-MB-231 cells (Fig. 2c). In MDA-MB-231 cells, the levels of p21 and TNF α proteins remained unaltered, while Maspin levels declined at 24 h (Fig. 2d). However, a 50% increase in TNF α levels was observed at 48h post infection (Fig. 2d). In MT1A2 cells, a two-fold increase in p21 levels and decline in Maspin and TNF α levels was evident at 24h (Fig. 2e). At 48 h, a decline in the expression levels of p21, Maspin and TNF α was noticed in MT1A2 cells. Additionally, the apoptosis-related Bok, Bax, Bmf and Puma proteins levels either declined or remained unaltered in both MDA-MB-231 and MT1A2 cells (Supplementary Fig. 2). These results suggest that cell-type-specific

differences in Bcl2 family pro-survival or pro-apoptotic protein expression levels contribute towards the induction of apoptosis in human or mouse mammary cancer cells.

For some of the proteins involved in the inhibition of tumorigenesis, the activation state rather than the expression level appears to be critical. Therefore, both the expression levels and the activation state of caspase 3, caspase 7 and PARP were examined by Western blot analyses of MDA-MB-231 or MT1A2 cells infected with HAd-EphrinA1-Fc using antibodies that differentiate between the full-length and cleaved products. In MT1A2 cells, both caspase 3 and caspase 7, the executioner caspases of apoptotic pathways, were found to be cleaved 24 h post-infection with HAd-EphrinA1-Fc (Fig. 3a). The reduction in the caspase 3 and the PARP proteins, a typical feature of caspase-dependent apoptosis, was also evident at 24 -72 h post-infection (Figs. 3a and 3b). The presence of cleaved caspases and PARP proteins suggest that HAd-EphrinA1-Fc could also directly induce apoptosis.

To validate if EphrinA1-Fc expression induces apoptosis *in vivo*, FVB-n mice bearing MT1A2-derived tumors were inoculated i.t. with HAd-EphrinA1-Fc or HAd- E1E3. The tumor tissues collected at seven days post-inoculation were analyzed by immunohistochemistry for expression of cleaved caspase 3 and PARP. Results specified increased expression of cleaved caspase 3 and PARP in tumor tissue sections indicating that EphrinA1-Fc also induced apoptosis *in vivo* (Fig. 3c). Altogether, the *in vitro* and *in vivo* evidences suggest the involvement of the post-translational regulatory mechanism/s in the induction of apoptosis by HAd-EphrinA1-Fc.

Single or multiple HAd-Ephrin-A1-Fc i.t. inoculations inhibit tumor growth

To determine the anti-tumor effects of EphrinA1-Fc expression during early tumorigenesis, FVB-n mice were inoculated with MT1A2 cells. One week after cell implantation, the mice were inoculated with one or three doses of 10^9 pfu of HAd-EphrinA1-Fc or HAd- E1E3 (Fig. 4). All control groups receiving one or three doses of PBS and empty vector showed similar tumor growth. In the one inoculation HAd-EphrinA1-Fc group, there was an approximately 52% inhibition in tumor growth compared to the empty vector control group by the end of the study (6 weeks post-inoculation) [Fig. 4 top]. The maximum inhibition in tumor growth was observed during the first week following inoculation with HAd-EphrinA1-Fc, but with time the inhibitory effect faded away. Indications are that a single injection of HAd-Ephrin-A1-Fc has an inhibitory growth effect only in the early stages of tumor growth. By the end of the study, the three inoculation HAd-EphrinA1-Fc group showed significant ($p < 0.05$) delay in tumor growth with an average of 75% reduction of tumor growth compared to the empty vector treated control group (Fig. 4 bottom). In addition, the three inoculations of HAd-EphrinA1-Fc showed a better tumor growth inhibitory effect than the single inoculation and closely approached statistical significance at various time points ($P < 0.1$). These results suggest that during the early stages of tumor growth, the therapeutic effect of EphrinA1-Fc can be enhanced by increasing the number of HAd-EphrinA1-Fc inoculations.

Effect of EphrinA1-Fc-EphA2 interaction-mediated apoptosis and Flt3L induced immunotherapy in developing an anti-tumor immune response

Flt3L is known to boost DC maturation and their migration thereby improving tumor-specific immune responses. HAd-Flt3L-infected cells clearly showed expression of Flt3L by Western blot analysis, and preliminary evidence is consistent with earlier reports [51] which indicate that there is an increase in the CD11c⁺ DC in the spleen and immunoreactivity in the tumors microenvironment of HAd-Flt3L-infected mice compared to empty vector infected mice (Supplementary Fig. 1d and 1e). Coupled with the significant anti-tumor effects of HAd-EphrinA1-Fc, this suggests that these two vectors used in combination could provide synergistic effects.

To investigate if EphrinA1-Fc-EphA2 interaction-mediated apoptosis would have an additive effect on Flt3L-induced tumor-specific T cell response, tumor bearing immunocompetent mice were inoculated i.t. with HAd- E1E3, HAd-EphrinA1-Fc, HAd-Flt3L, or a combination of HAd-EphrinA1-Fc and HAd-Flt3L. The spleens were collected at Day 45 post-inoculation. Total splenocytes were used in an ELISpot assay to monitor the induction of IFN- γ expression upon stimulation. There was a significant ($P < 0.05$) increase in the number of IFN- γ secreting splenocytes in the HAd-EphrinA1-Fc + HAd-Flt3L group compared to the HAd- E1E3 or HAd-EphrinA1-Fc groups, while the HAd-Flt3L group was marginally significant ($P = 0.07$) compared to HAd- E1E3 group. In addition, the differences between HAd-Flt3L and the combination group were not significant ($P = 0.37$) indicating the enhancement of a tumor-specific T cell response was largely due to HAd-Flt3L treatment (Fig. 5a).

Splenocytes were also used to positively select CD8⁺ T cells for cytotoxicity assay. The cytotoxicity due to the tumor-specific cytotoxic CD8⁺ T cells in the HAd-EphrinA1-Fc, HAd-Flt3L, or HAd-EphrinA1-Fc + HAd-Flt3L groups was significantly higher compared to the HAd- E1E3 or PBS groups (Fig. 5b). There was an appreciable average increase of about 28% and 67% in the cytotoxicity in the combination group compared to the HAd-Flt3L or HAd-EphrinA1-Fc groups, respectively, although the data were not statistically significant. The results suggest that a combination of EphrinA1-Fc and Flt3L expression in the tumor tissue boosted the development of a tumor-specific T cell response.

Effect of EphrinA1-Fc-EphA2 interaction-mediated apoptosis and Flt3L-induced immunotherapy in inhibiting tumor growth

To investigate whether a synergistic effect of EphrinA1-Fc-EphA2 interaction-mediated apoptosis and Flt3L-induced immunotherapy would have an enhanced inhibition on the growth of established tumors, tumor-bearing FVB-n mice were inoculated i.t with one or three doses of HAd- E1E3, HAd-EphrinA1-Fc, HAd-Flt3L, or a combination of HAd-EphrinA1-Fc and HAd-Flt3L (Fig. 6). The tumors in the control mice grew uninhibited to reach an average size of 616 mm³ by the end of the study. In the PBS or HAd- E1E3 one inoculation groups, no appreciable difference in tumor growth was detected (Fig. 6 top). The HAd-EphrinA1-Fc or HAd-Flt3L one or three inoculation groups showed an approximate 51% decline in tumor growth compared to the empty vector control groups by the end of the

study (5 weeks post-inoculation) (Fig. 6 top and bottom). The most prominent decreases in tumor growth were observed during the first three weeks post-inoculation.

The HAd-EphrinA1-Fc + HAd-Flt3L one or three inoculation groups showed an approximate 56 or 69% decline in tumor growth, respectively, compared to the empty vector groups, and an approximate 60 or 80% decline, respectively, compared to the mock groups by the end of the study. The HAd-EphrinA1-Fc + HAd-Flt3L groups had increased inhibition in tumor growth compared to the HAd-EphrinA1-Fc or HAd-Flt3L groups at various time points, but the differences were not statistically significant. It is noteworthy that during the time course of our experiments we did not observe any mortality either in the untreated tumor-bearing mice or in the groups receiving single or three i.t. inoculations of HAd-EphrinA1-Fc or HAd-Flt3L. Once the mice were sacrificed, HAd vector-associated changes in liver were observed upon histopathological examination, as reported previously [52]. While none of the mice became tumor free in the HAd-EphrinA1-Fc group, the results indicated that the HAd-EphrinA1-Fc inoculations functioned better in non-palpable tumors (75% reduction) compared to palpable tumors (51% reduction), and that the therapeutic efficacy could be enhanced by multiple injections.

DISCUSSION

Development of therapeutic strategies using Ad vector-mediated transgene overexpression has demonstrated great promise in breast cancers [53] since the conventional approaches for breast cancer treatment are not very effective against the metastatic spread and recurrence of the disease [54]. Efficacy of anti-cancer therapies may be enhanced by combining molecular therapies to induce tumor-specific immune responses. We have previously demonstrated that Ad-mediated EphrinA1 expression in cancer cells inhibits proliferation and reduces tumorigenicity [21,22]. We have extended these findings in an immunocompetent mouse model of breast cancer to report that EphrinA1-Fc expression in breast cancer-derived cells induces apoptosis and that multiple inoculations with HAd-EphrinA1-Fc significantly inhibit tumor growth. Additionally, Flt3L expression in the tumor tissue induces an anti-tumor immune response. The anti-tumor effect of HAd-EphrinA1-Fc is augmented when used in combination with HAd-Flt3L.

EphrinA1 regulates EphA2 overexpression by inducing EphA2 phosphorylation and endocytic degradation [21,55]. EphA2 overexpression is implicated in the development of breast, prostate, urinary bladder, glioma, melanoma and other cancers [10,11]. Our *in vitro* studies indicate that EphrinA1-Fc expression results in the induction of apoptosis primarily in breast cancer cells. We analyzed the changes in protein expression levels of several pro- or anti- apoptosis-related proteins but the mechanisms appear to be different with respect to the timing, potency and involvement of intermediary signaling molecules of apoptotic signaling cascades. The reduced expression of Bcl-2 protein levels suggests the importance of Bcl-2 in inducing the apoptosis of MDA-MB-231 and MT1A2 cells. The cleavage of caspase 3 and PARP proteins indicates that an impaired DNA repair mechanism is associated with the induction of apoptosis. An imbalance in the equilibrium between the Bcl-2 family proteins may enhance the sensitivity of cancer cells towards apoptosis through a mitochondrial death cascade, or the upregulation of TNF α suggests that intrinsic pathway

may also be important. It is likely that both these pathways are linked and changes in one pathway influence the other as previously suggested [56]. The alterations in caspases and PARP proteins clearly indicate that such changes in intermediate signaling molecules have converged to a common pathway leading to apoptosis. We, therefore, suggest the significance of both the intrinsic and extrinsic pathways in the induction of apoptosis by EphrinA1 in breast cancers. Additionally, since induction of apoptosis is associated with a substantial reduction in protein synthesis in several cell types [57], the decline in pro-apoptotic protein expression observed in our study suggests that exposure to HAd-EphrinA1-Fc-mediated apoptotic stimuli might have also led to an inhibition of protein synthesis. However, the precise mechanisms of HAd-EphrinA1-Fc induced apoptosis need to be further elucidated.

Earlier we demonstrated that MT1A2 cells infected with HAd-EphrinA1-Fc failed to establish tumors in the FVB-n mouse model [22]. The purpose of initiating a HAd-EphrinA1-Fc inoculation before the development of palpable tumors was to intercept a tumor at an early stage of development. A single inoculation of HAd-EphrinA1-Fc did delay the tumor growth. In addition, the three inoculations of HAd-EphrinA1-Fc produced an improved inhibitory effect on tumor growth compared to the single inoculation. In non-palpable tumors, HAd-EphrinA1-Fc produced better results than in palpable tumors. The most notable delay in tumor growth was observed with the combination regimen of HAd-EphrinA1-Fc and HAd-Flt3L suggesting that Flt3L may additively function with EphrinA1 in palpable/established tumors due to the development of an anti-tumor cytotoxic T cell response. These data suggest that the use of a third Ad vector, possibly a nonhuman Ad vector expressing EphrinA1-Fc, should provide further inhibition or reduction in the tumor size. Use of additional transgenes that target different apoptosis pathways should improve upon EphrinA1- and Flt3L-based cancer therapy.

The EphA2 receptor tyrosine kinase has been reported to function in both tumor progression as well as suppression [9]. While the majority of emerging evidence indicates that EphA2 functions in tumor progression, there is also evidence that it is dependent on the genomic context of the cell in addition to the presence or absence of Ephrin ligands. In the genomic context, EphA2 deficiency suppressed mammary tumorigenesis and metastasis in ErbB2 (Her2) overexpressing mouse mammary tumor virus (MMTV) long terminal repeat-driven MMTV-Neu (rat homolog of ErbB2) transgenic mice but not in the polyomavirus middle T antigen overexpressing MMTV-PyV-mT transgenic mice [18]. EphA2 promoted mammary adenocarcinoma tumorigenesis and metastatic progression in mice by amplifying ErbB2 signaling, and the MMTV-Neu mice also showed enhanced sensitivity towards an anti-EphA2 targeted monoclonal antibody therapy. On the other hand, the MMTV-PyV-mT mice derived MT1A2 cell tumors in syngeneic FVB/n mice showed a marked effect in reducing tumor growth when treated with EphrinA1-Fc [22]. While EphA2 physically interacts with ErbB2, the downstream signaling may be different in a genomic context lacking over-expressed ErbB2 and in the presence or absence of Ephrin ligands. Recently, expression levels of Eph receptors and Ephrin ligands have shown significant correlations with clinical outcomes in microarray datasets [58]. Interestingly, EphrinA1 and EphA2 co-expression was observed in patients with breast cancer recurrence, while a mutually exclusive pattern

was observed in lymph node metastasis indicating the importance of EphrinA1 expression pattern in breast cancer prognosis.

The heterogeneity presented by tumors in terms of genetic background and oncogenic alterations precludes a single therapeutic modality to be fully effective in aggressive and metastatic cancers [2,54]. While, complete secession of tumor growth was not achieved with the combination of HAd-EphrinA1-Fc + HAd-Flt3L, the tumors did show significant delay in growth during our examination period. This could be due to the high early transgene expression by these vectors within MT1A2 tumors but transient persistence of the vector leading to its gradual decline and systemic clearance may be responsible for the failure in sustained effect [59]. However, we did observe an enhanced adaptive immune response against the tumors with the combination therapy even though the inoculation of MT1A2 cells on the contra-lateral side did not eliminate this tumor burden as revealed in the autopsy of the mice after the experiment. In addition, we could not monitor a second tumor progression on the contra-lateral side due to the enlargement of the first tumor to the pre-defined size limit. It is possible that the tumor growth inhibition via T cell response only persisted transiently. The loss of tumor-associated antigens and the development of a tumor phenotype that escapes the T cell response might have contributed to the incomplete tumor regression observed in our study.

Other mechanisms such as alterations in immune cell recognizing MHC molecules on tumor cell surface [60] may also explain this phenomenon. The involvement of regulatory T cells (Tregs) in the development of immune tolerance is also possible. A higher frequency of Tregs has been identified in the peripheral blood of breast cancer patients when compared to healthy controls [61]. Tregs have also been identified in the tumor microenvironment and draining lymph nodes and have influenced cancer prognosis [62]. Further characterization of the tumor microenvironment and MT1A2 cells isolated from the tumor-bearing treated mice will be worth pursuing to support or refute this phenomenon. In the FVB/n mouse model of breast cancer, the metastasis was not observed. There is a need to evaluate our combinational approach in a metastatic immunocompetent animal model to determine whether it will prevent metastasis.

The capability of cancer cells to obviate the immunosurveillance (innate and adaptive immune response) by the selection of non-immunogenic variants is now regarded as one of the hallmarks of cancer [63]. Recently, in a glioblastoma multiforme mice model, combined use of Ad expressing herpes simplex virus-type 1 thymidine kinase gene and Flt3L led to anti-brain tumor-specific immunity and the generation of immunological memory [64]. The use of EphrinA1 conjugated to albumin microspheres showed inhibition of *in vitro* lung cancer cell growth and migration [65]. Our results in a mouse model of breast cancer indicate that a combination of EphrinA1 and Flt3L with repeated administration elicits an anti-tumor immune response suggesting that a combination of immunostimulatory molecules will be advantageous in cancer-directed cytotoxic therapies. Following the lysis of cancer cells, the tumor antigens may be phagocytosed by DC for antigenic presentation to T cells. A more detailed characterization of tumor-associated T cells, DC and NK cells is warranted to further validate the mechanisms of anti-tumor effects of this type of combination therapy.

Supplementary Material

Refer to Web version on PubMed Central for supplementary material.

Acknowledgments

This work was supported by Public Health Service grant CA110176 from the National Cancer Institute. We thank Jane Kovach for her excellent secretarial assistance and Ahmed Mohamed for help with statistical analyses.

References

1. Anderson WF, Matsuno R. Breast cancer heterogeneity: a mixture of at least two main types? *J Natl Cancer Inst.* 2006; 98:948–951.10.1093/jnci/djj295 [PubMed: 16849671]
2. Joyce JA, Pollard JW. Microenvironmental regulation of metastasis. *Nat Rev Cancer.* 2009; 9:239–252.10.1038/nrc2618 [PubMed: 19279573]
3. Hanahan D, Weinberg RA. The hallmarks of cancer. *Cell.* 2000; 100:57–70. [PubMed: 10647931]
4. Elmore S. Apoptosis: a review of programmed cell death. *Toxicol Pathol.* 2007; 35:495–516. [PubMed: 17562483]
5. Kasibhatla S, Tseng B. Why target apoptosis in cancer treatment? *Mol Cancer Ther.* 2003; 2:573–580. [PubMed: 12813137]
6. Okada H, Mak TW. Pathways of apoptotic and non-apoptotic death in tumour cells. *Nat Rev Cancer.* 2004; 4:592–603. [PubMed: 15286739]
7. Taylor ST, Hickman JA, Dive C. Survival signals within the tumour microenvironment suppress drug-induced apoptosis: lessons learned from B lymphomas. *Endocr Relat Cancer.* 1999; 6:21–23. [PubMed: 10732782]
8. Fesik SW. Promoting apoptosis as a strategy for cancer drug discovery. *Nat Rev Cancer.* 2005; 5:876–885. [PubMed: 16239906]
9. Tandon M, Vemula SV, Mittal SK. Emerging strategies for EphA2 receptor targeting for cancer therapeutics. *Expert Opin Ther Targets.* 2011; 15:31–51.10.1517/14728222.2011.538682 [PubMed: 21142802]
10. Pasquale EB. Eph receptors and ephrins in cancer: bidirectional signalling and beyond. *Nat Rev Cancer.* 2010; 10:165–180.10.1038/nrc2806 [PubMed: 20179713]
11. Wykosky J, Debinski W. The EphA2 receptor and ephrinA1 ligand in solid tumors: function and therapeutic targeting. *Mol Cancer Res.* 2008; 6:1795–1806.10.1158/1541-7786.MCR-08-0244 [PubMed: 19074825]
12. Zelinski DP, Zantek ND, Stewart JC, Irizarry AR, Kinch MS. EphA2 overexpression causes tumorigenesis of mammary epithelial cells. *Cancer Res.* 2001; 61:2301–2306. [PubMed: 11280802]
13. Bruckheimer EM, Fazenbaker CA, Gallagher S, et al. Antibody-dependent cell-mediated cytotoxicity effector-enhanced EphA2 agonist monoclonal antibody demonstrates potent activity against human tumors. *Neoplasia.* 2009; 11:509–17. [PubMed: 19484140]
14. Coffman KT, Hu M, Carles-Kinch K, et al. Differential EphA2 epitope display on normal versus malignant cells. *Cancer Res.* 2003; 63:7907–7912. [PubMed: 14633720]
15. Lee JW, Han HD, Shahzad MM, et al. EphA2 immunoconjugate as molecularly targeted chemotherapy for ovarian carcinoma. *J Natl Cancer Inst.* 2009; 101:1193–1205.10.1093/jnci/djp23 [PubMed: 19641174]
16. Wykosky J, Gibo DM, Debinski W. A novel, potent, and specific ephrinA1-based cytotoxin against EphA2 receptor expressing tumor cells. *Mol Cancer Ther.* 2007; 6:3208–3218.10.1158/1535-7163.MCT-07-0200 [PubMed: 18089715]
17. Zhuang G, Brantley-Sieders DM, Vaught D, et al. Elevation of receptor tyrosine kinase EphA2 mediates resistance to trastuzumab therapy. *Cancer Res.* 2010; 70:299–308.10.1158/0008-5472.CAN-09-1845 [PubMed: 20028874]

18. Brantley-Sieders DM, Zhuang G, Hicks D, et al. The receptor tyrosine kinase EphA2 promotes mammary adenocarcinoma tumorigenesis and metastatic progression in mice by amplifying ErbB2 signaling. *J Clin Invest.* 2008; 118:64–78.10.1172/JCI33154 [PubMed: 18079969]
19. Alves PM, Faure O, Graff-Dubois S, et al. EphA2 as target of anticancer immunotherapy: identification of HLA-A*0201-restricted epitopes. *Cancer Res.* 2003; 63:8476–8480. [PubMed: 14679012]
20. Wesa AK, Herrem CJ, Mandic M, et al. Enhancement in specific CD8+ T cell recognition of EphA2+ tumors in vitro and in vivo after treatment with ligand agonists. *J Immunol.* 2008; 181:7721–7727. [PubMed: 19017961]
21. Noblitt LW, Bangari DS, Shukla S, et al. Decreased tumorigenic potential of EphA2-overexpressing breast cancer cells following treatment with adenoviral vectors that express EphrinA1. *Cancer Gene Ther.* 2004; 11:757–766.10.1038/sj.cgt.7700761 [PubMed: 15359289]
22. Noblitt LW, Bangari DS, Shukla S, Mohammed S, Mittal SK. Immunocompetent mouse model of breast cancer for preclinical testing of EphA2-targeted therapy. *Cancer Gene Ther.* 2005; 12:46–53.10.1038/sj.cgt.7700763 [PubMed: 15486559]
23. McKenna HJ, Stocking KL, Miller RE, et al. Mice lacking flt3 ligand have deficient hematopoiesis affecting hematopoietic progenitor cells, dendritic cells, and natural killer cells. *Blood.* 2000; 95:3489–3497. [PubMed: 10828034]
24. Hannum C, Culpepper J, Campbell D, et al. Ligand for FLT3/FLK2 receptor tyrosine kinase regulates growth of haematopoietic stem cells and is encoded by variant RNAs. *Nature.* 1994; 368:643–648.10.1038/368643a0 [PubMed: 8145851]
25. Watowich SS, Liu YJ. Mechanisms regulating dendritic cell specification and development. *Immunol Rev.* 2010; 238:76–92. [PubMed: 20969586]
26. Stirewalt DL, Radich JP. The role of FLT3 in haematopoietic malignancies. *Nat Rev Cancer.* 2003; 3:650–665. [PubMed: 12951584]
27. Lindberg RA, Hunter T. cDNA cloning and characterization of eck, an epithelial cell receptor protein-tyrosine kinase in the eph/elk family of protein kinases. *Mol Cell Biol.* 1990; 10:6316–6324. [PubMed: 2174105]
28. de Saint-Vis B, Bouchet C, Gautier G, et al. Human dendritic cells express neuronal Eph receptor tyrosine kinases: role of EphA2 in regulating adhesion to fibronectin. *Blood.* 2003; 102:4431–4440. [PubMed: 12907451]
29. Lynch DH, Andreassen A, Maraskovsky E, et al. Flt3 ligand induces tumor regression and antitumor immune responses in vivo. *Nat Med.* 1997; 3:625–631. [PubMed: 9176488]
30. Maraskovsky E, Brasel K, Teepe M, et al. Dramatic increase in the numbers of functionally mature dendritic cells in Flt3 ligand-treated mice: multiple dendritic cell subpopulations identified. *J Exp Med.* 1996; 184:1953–1962. [PubMed: 8920882]
31. Chen K, Braun S, Lyman S, et al. Antitumor activity and immunotherapeutic properties of Flt3-ligand in a murine breast cancer model. *Cancer Res.* 1997; 57:3511–3516. [PubMed: 9270021]
32. Marroquin CE, Westwood JA, Lapointe R, et al. Mobilization of dendritic cell precursors in patients with cancer by flt3 ligand allows the generation of higher yields of cultured dendritic cells. *J Immunother.* 2002; 25:278–288. [PubMed: 12000870]
33. Talmadge JE, Donkor M, Scholar E. Inflammatory cell infiltration of tumors: Jekyll or Hyde. *Cancer Metastasis Rev.* 2007; 26:373–400.10.1007/s10555-007-9072-0 [PubMed: 17717638]
34. Bingle L, Brown NJ, Lewis CE. The role of tumour-associated macrophages in tumour progression: implications for new anticancer therapies. *J Pathol.* 2002; 196:254–265.10.1002/path.1027 [PubMed: 11857487]
35. Chakravarty PK, Alfieri A, Thomas EK, et al. Flt3-ligand administration after radiation therapy prolongs survival in a murine model of metastatic lung cancer. *Cancer Res.* 1999; 59:6028–6032. [PubMed: 10626784]
36. Chakravarty PK, Guha C, Alfieri A, et al. Flt3L therapy following localized tumor irradiation generates long-term protective immune response in metastatic lung cancer: its implication in designing a vaccination strategy. *Oncology.* 2006; 70:245–254.10.1159/000096288 [PubMed: 17047396]

37. Averbook BJ, Schuh JL, Papay R, Maliszewski C. Antitumor effects of Flt3 ligand in transplanted murine tumor models. *J Immunother.* 2002; 25:27–35. [PubMed: 11924908]
38. Saito T, Takayama T, Osaki T, et al. Combined mobilization and stimulation of tumor-infiltrating dendritic cells and natural killer cells with Flt3 ligand and IL-18 in vivo induces systemic antitumor immunity. *Cancer Sci.* 2008; 99:2028–2036.10.1111/j.1349-7006.2008.00907.x [PubMed: 19016763]
39. Bernt KM, Ni S, Tieu AT, Lieber A. Assessment of a combined, adenovirus-mediated oncolytic and immunostimulatory tumor therapy. *Cancer Res.* 2005; 65:4343–4352.10.1158/0008-5472.CAN-04-3527 [PubMed: 15899826]
40. Curtin JF, Liu N, Candolfi M, et al. HMGB1 mediates endogenous TLR2 activation and brain tumor regression. *PLoS Med.* 2009; 6:e10.10.1371/journal.pmed.1000010 [PubMed: 19143470]
41. Hou S, Kou G, Fan X, et al. Eradication of hepatoma and colon cancer in mice with Flt3L gene therapy in combination with 5-FU. *Cancer Immunol Immunother.* 2007; 56:1605–1613.10.1007/s00262-007-0306-3 [PubMed: 17361437]
42. King GD, Kroeger KM, Bresee CJ, et al. Flt3L in combination with HSV1-TK-mediated gene therapy reverses brain tumor-induced behavioral deficits. *Mol Ther.* 2008; 16:682–690.10.1038/mt.2008.18 [PubMed: 18283279]
43. King GD, Muhammad AK, Curtin JF, et al. Flt3L and TK gene therapy eradicate multifocal glioma in a syngeneic glioblastoma model. *Neuro Oncol.* 2008; 10:19–31.10.1215/15228517-2007-045 [PubMed: 18079358]
44. Puntel M, Muhammad AG, Candolfi M, et al. A novel bi-cistronic high-capacity gutless adenovirus vector driving constitutive expression of HSV1-TK and Tet-inducible expression of Flt3L for glioma therapeutics. *J Virol.* 2010; 84:6007–6017.10.1128/JVI.00398-10 [PubMed: 20375153]
45. van Olphen AL, Mittal SK. Development and characterization of bovine x human hybrid cell lines that efficiently support the replication of both wild-type bovine and human adenoviruses and those with E1 deleted. *J Virol.* 2002; 76:5882–5892. [PubMed: 12021321]
46. Addison CL, Braciak T, Ralston R, et al. Intratumoral injection of an adenovirus expressing interleukin 2 induces regression and immunity in a murine breast cancer model. *Proc Natl Acad Sci U S A.* 1995; 92:8522–8526. [PubMed: 7667323]
47. Ng P, Parks RJ, Cummings DT, et al. A high-efficiency Cre/loxP-based system for construction of adenoviral vectors. *Hum Gene Ther.* 1999; 10:2667–2672.10.1089/10430349950016708 [PubMed: 10566894]
48. Sharma A, Bangari DS, Tandon M, et al. Comparative analysis of vector biodistribution, persistence and gene expression following intravenous delivery of bovine, porcine and human adenoviral vectors in a mouse model. *Virology.* 2009; 386:44–54.10.1016/j.virol.2009.01.008 [PubMed: 19211122]
49. Sharma A, Tandon M, Ahi YS, et al. Evaluation of cross-reactive cell-mediated immune responses among human, bovine and porcine adenoviruses. *Gene Ther.* 2010; 17:634–642.10.1038/gt.2010.1 [PubMed: 20164856]
50. Ghulam Muhammad AK, Candolfi M, King GD, et al. Antiglioma immunological memory in response to conditional cytotoxic/immune-stimulatory gene therapy: humoral and cellular immunity lead to tumor regression. *Clin Cancer Res.* 2009; 15:6113–6127. [PubMed: 19789315]
51. Miller G, Pillarisetty VG, Shah AB, Lahrs S, DeMatteo RP. Murine Flt3 ligand expands distinct dendritic cells with both tolerogenic and immunogenic properties. *J Immunol.* 2003; 170:3554–3564. [PubMed: 12646617]
52. Sharma A, Bangari DS, Tandon M, HogenEsch H, Mittal SK. Evaluation of innate immunity and vector toxicity following inoculation of bovine, porcine or human adenoviral vectors in a mouse model. *Virus Res.* 2010; 153:134–142. [PubMed: 20659505]
53. Sharma A, Tandon M, Bangari DS, Mittal SK. Adenoviral vector-based strategies for cancer therapy. *Curr Drug ther.* 2009; 4:117–138. [PubMed: 20160875]
54. Kitano H. Cancer as a robust system: implications for anticancer therapy. *Nat Rev Cancer.* 2004; 4:227–235. [PubMed: 14993904]

55. Carles-Kinch K, Kilpatrick KE, Stewart JC, Kinch MS. Antibody targeting of the EphA2 tyrosine kinase inhibits malignant cell behavior. *Cancer Res.* 2002; 62:2840–2847. [PubMed: 12019162]
56. Igney FH, Krammer PH. Death and anti-death: tumour resistance to apoptosis. *Nat Rev Cancer.* 2002; 2:277–288. [PubMed: 12001989]
57. Clemens MJ, Bushell M, Jeffrey IW, Pain VM, Morley SJ. Translation initiation factor modifications and the regulation of protein synthesis in apoptotic cells. *Cell Death Differ.* 2000; 7:603–615. [PubMed: 10889505]
58. Brantley-Sieders DM, Jiang A, Sarma K, et al. Eph/Ephrin Profiling in Human Breast Cancer Reveals Significant Associations between Expression Level and Clinical Outcome. *PLoS One.* 2011; 6:e24426. [PubMed: 21935409]
59. Tandon M, Sharma A, Vemula SV, Bangari DS, Mittal SK. Sequential administration of bovine and human adenovirus vectors to overcome vector immunity in an immunocompetent mouse model of breast cancer. *Virus Res.* 2011
60. Campoli M, Ferrone S. Tumor escape mechanisms: potential role of soluble HLA antigens and NK cells activating ligands. *Tissue Antigens.* 2008; 72:321–334. [PubMed: 18700879]
61. Horlock C, Stott B, Dyson PJ, et al. The effects of trastuzumab on the CD4+CD25+FoxP3+ and CD4+IL17A+ T-cell axis in patients with breast cancer. *Br J Cancer.* 2009; 100:1061–1067. [PubMed: 19277040]
62. Galon J, Costes A, Sanchez-Cabo F, et al. Type, density, and location of immune cells within human colorectal tumors predict clinical outcome. *Science.* 2006; 313:1960–1964. [PubMed: 17008531]
63. Zitvogel L, Tesniere A, Kroemer G. Cancer despite immunosurveillance: immunoselection and immunosubversion. *Nat Rev Immunol.* 2006; 6:715–727. [PubMed: 16977338]
64. King GD, Muhammad AG, Larocque D, et al. Combined Flt3L/TK Gene Therapy Induces Immunological Surveillance Which Mediates an Immune Response Against a Surrogate Brain Tumor Neoantigen. *Mol Ther.* 2011; 19:1793–1801. [PubMed: 21505426]
65. Lee HY, Mohammed KA, Peruvemba S, Goldberg EP, Nasreen N. Targeted lung cancer therapy using ephrinA1-loaded albumin microspheres. *J Pharm Pharmacol.* 2011; 63:1401–1410. [PubMed: 21988421]

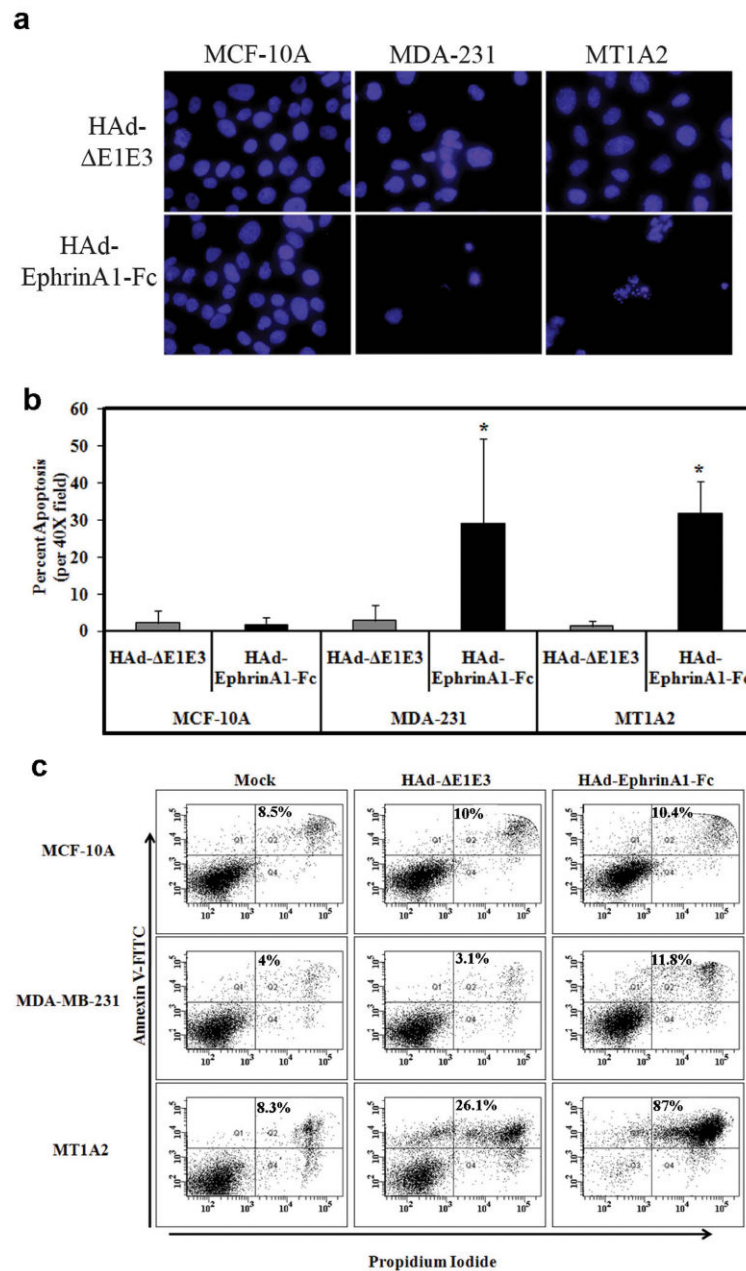


Figure 1. Adenovirus vector-mediated EphrinA1 expression induces apoptosis in cancer cells (a) MCF-10A, MDA-MB-231 and MT1A2 cells were infected with 100 pfu/cell of either HAd- E1E3 or HAd-EphrinA1-Fc. At 48 h post-infection, the cells were fixed, permeabilized and stained with DAPI to be examined for nuclear morphology under a fluorescence microscope. The nuclei were observed to be condensed and fragmented in MDA-MB-231 and MT1A2 cells. (b) The number of normal, condensed or fragmented nuclei was counted in six random fields at 40 \times magnification. (c) MCF-10A, MDA-MB-231 and MT1A2 cells were either mock-infected or infected with 100 pfu/cell of HAd- E1E3 or HAd-EphrinA1Fc. At 48 h post-infection, the cells were labeled with Annexin V-FITC and propidium iodide and analyzed by flow cytometry.

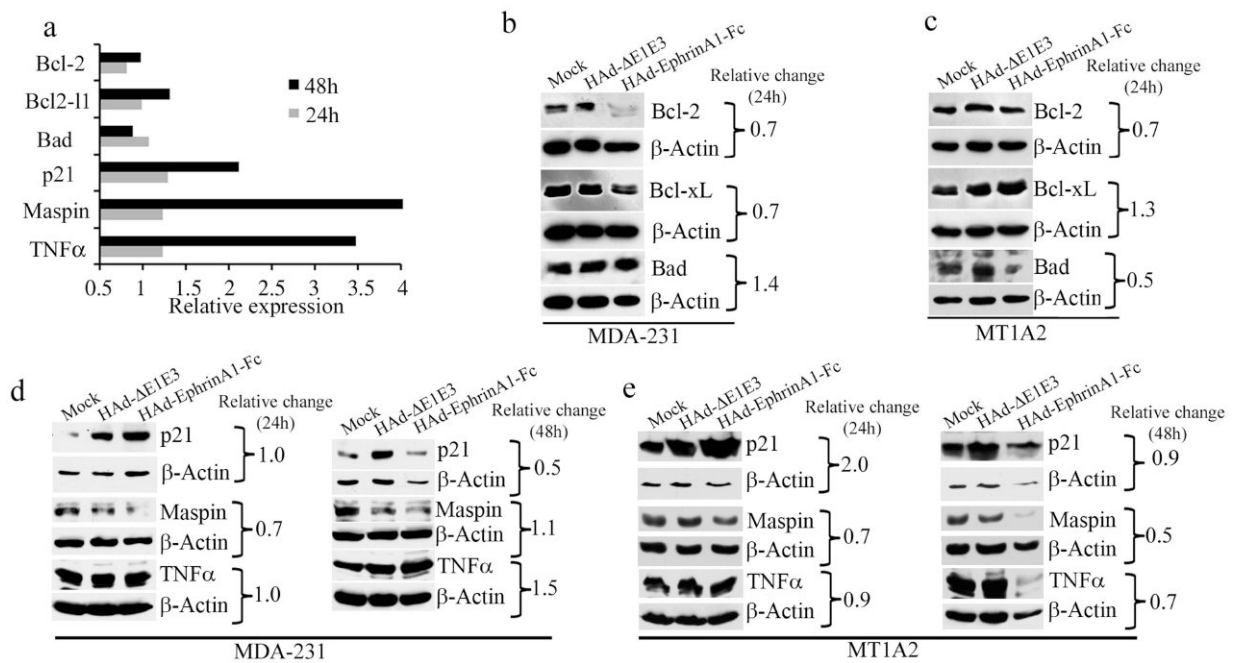


Figure 2. Adenovirus vector-mediated EphrinA1 expression modulates apoptosis-related gene and protein expression

(a) MDA-MB-231 cells were either mock-infected or infected with 100 pfu/cell of HAd-E1E3 or HAd-EphrinA1-Fc. Total RNA was isolated at 24 h or 48 h post-infection and was used to determine the expression levels of apoptosis-related genes by real-time RT-PCR using a gene array. The gene expression levels were normalized with three internal control genes (β -Actin, GAPDH and RPL13A). The relative change in gene expression for HAd-EphrinA1-Fc treated cells with respect to HAd-E1E3 control vector is shown. (b, c) MDA-MB-231 or MT1A2 cells were either mock-infected or infected with 100 pfu/cell of HAd-E1E3 or HAd-EphrinA1-Fc. At 24 h post-infection, whole cell lysates were prepared for Western blot analyses to determine expression levels of Bcl-2, Bcl-xl and Bad. (d, e) MDA-MB-231 or MT1A2 cells were either mock-infected or infected with 100 pfu/cell of HAd-E1E3 or HAd-EphrinA1-Fc. At 24 h and 48 h post-infection, whole cell lysates were prepared for Western blot analyses to determine expression levels of p21, maspin, and TNF- α . An antibody against β -Actin was used as a loading control. The relative change in the protein expression of HAd-EphrinA1-Fc treated cells compared to HAd-E1E3 treated cells is shown.

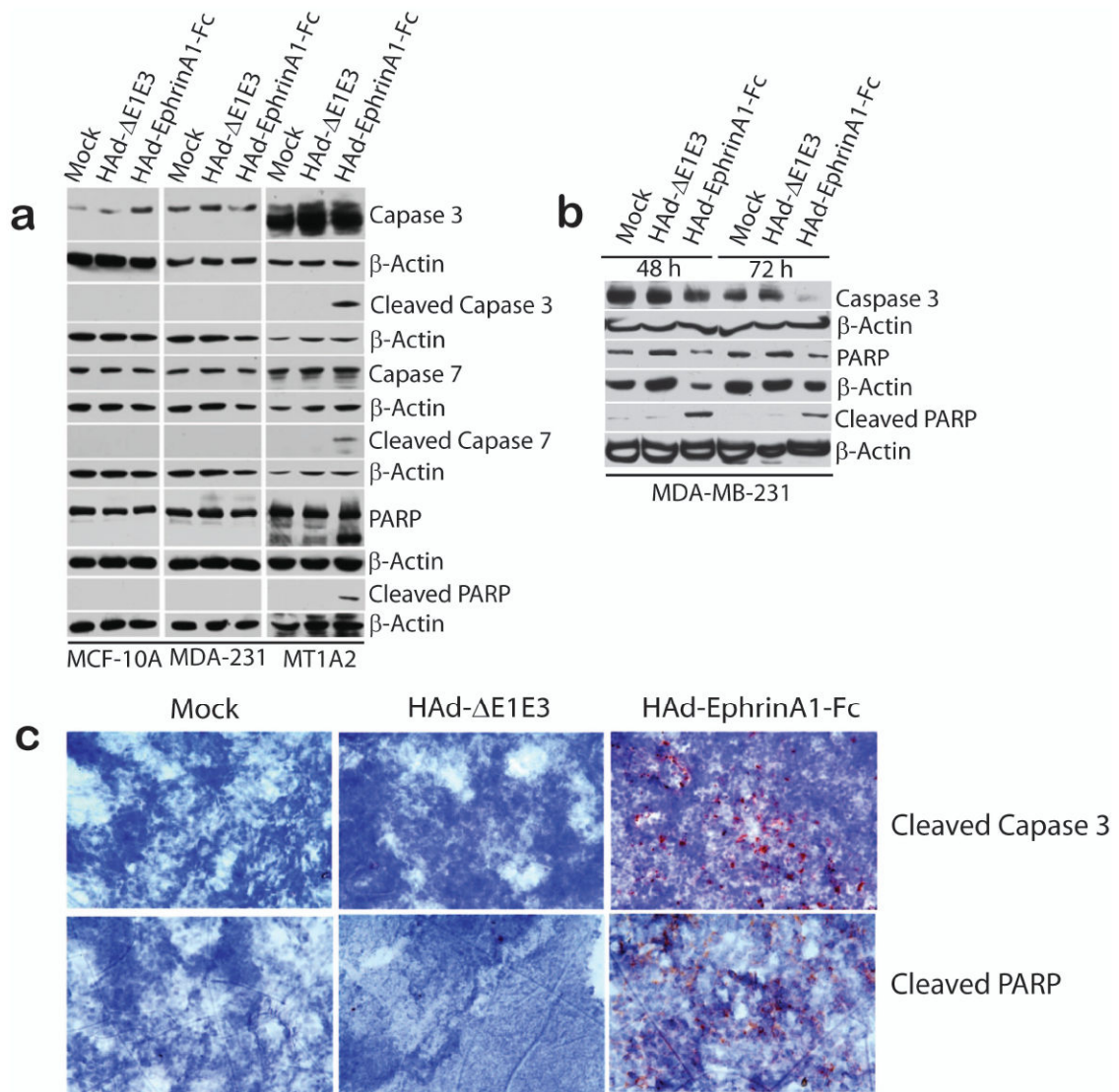


Figure 3. Activation of caspase 3, caspase 7 and PARP in breast cancer cells in response to EphrinA1 expression

(a) MCF-10A, MDA-MB-231 and MT1A2 cells were either mock-infected or infected with 100 pfu/cell of HAd- E1E3 or HAd-EphrinA1-Fc. At 24 h post-infection, whole cell lysates were prepared for Western blot analyses for full-length caspase 3, caspase 7 and PARP or the cleaved-forms of caspase 3, caspase 7 and PARP. An antibody against β -actin was used as an internal control. (b) In MDA-MB-231 cells, expression levels of caspase 3, PARP and cleaved PARP proteins were examined at 48 and 72 h post infection. (c) The tumor-bearing FVB/n mice were inoculated with PBS, HAd- E1E3 or HAd-EphrinA1-Fc. At Day 7 post-inoculation, mice were euthanized; the tumor tissues were collected and analyzed by immunohistochemistry with anti-cleaved caspase 3 or anti-cleaved PARP antibody.

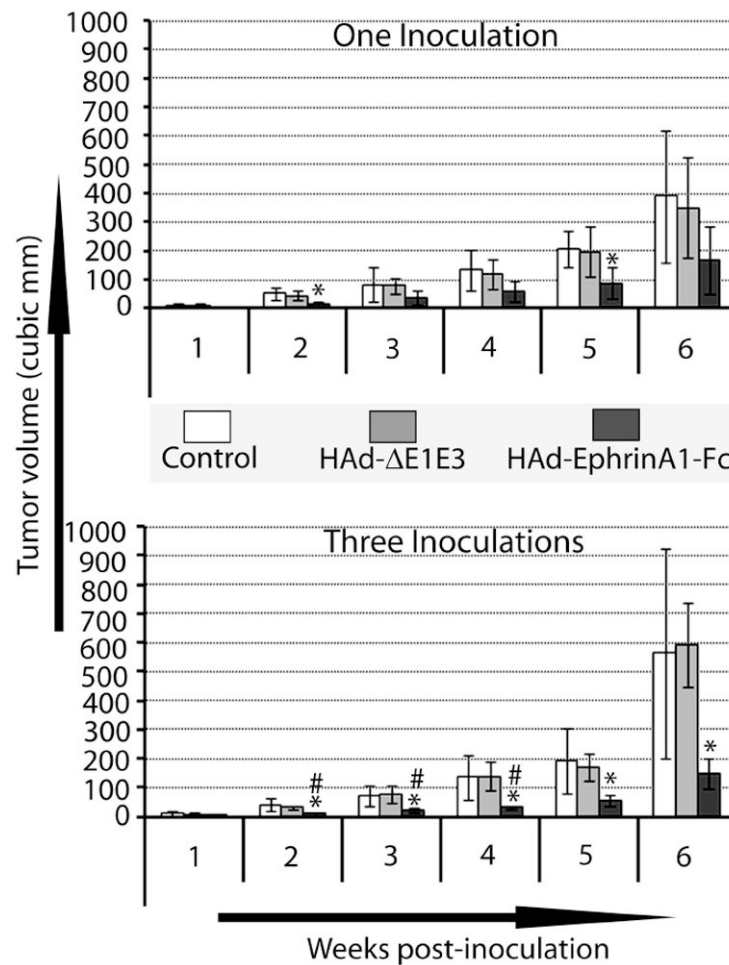


Figure 4. Inhibition in tumor growth in response to one or three i.t. inoculations of HAd-EphrinA1-Fc in non-palpable tumors

MT1A2 cells were implanted s.c. into the axillary region of FVB/n mice (n=8 per group). One week after cell implantation, animals were either mock-inoculated or inoculated with HAd- E1E3 or HAd-EphrinA1-Fc. The three inoculation group received three inoculations with a three day interval between inoculations. The tumor growth was monitored by Vernier caliper measurements at regular intervals, and the tumor volume was calculated by the formula $[\text{length} \times (\text{width})^2]/2$. * P<0.05 derived from ANOVA with Tukey's adjustments compared to the empty vector (HAd- E1E3) control, #, P<0.1 derived from unpaired t test compared to single i.t. inoculation.

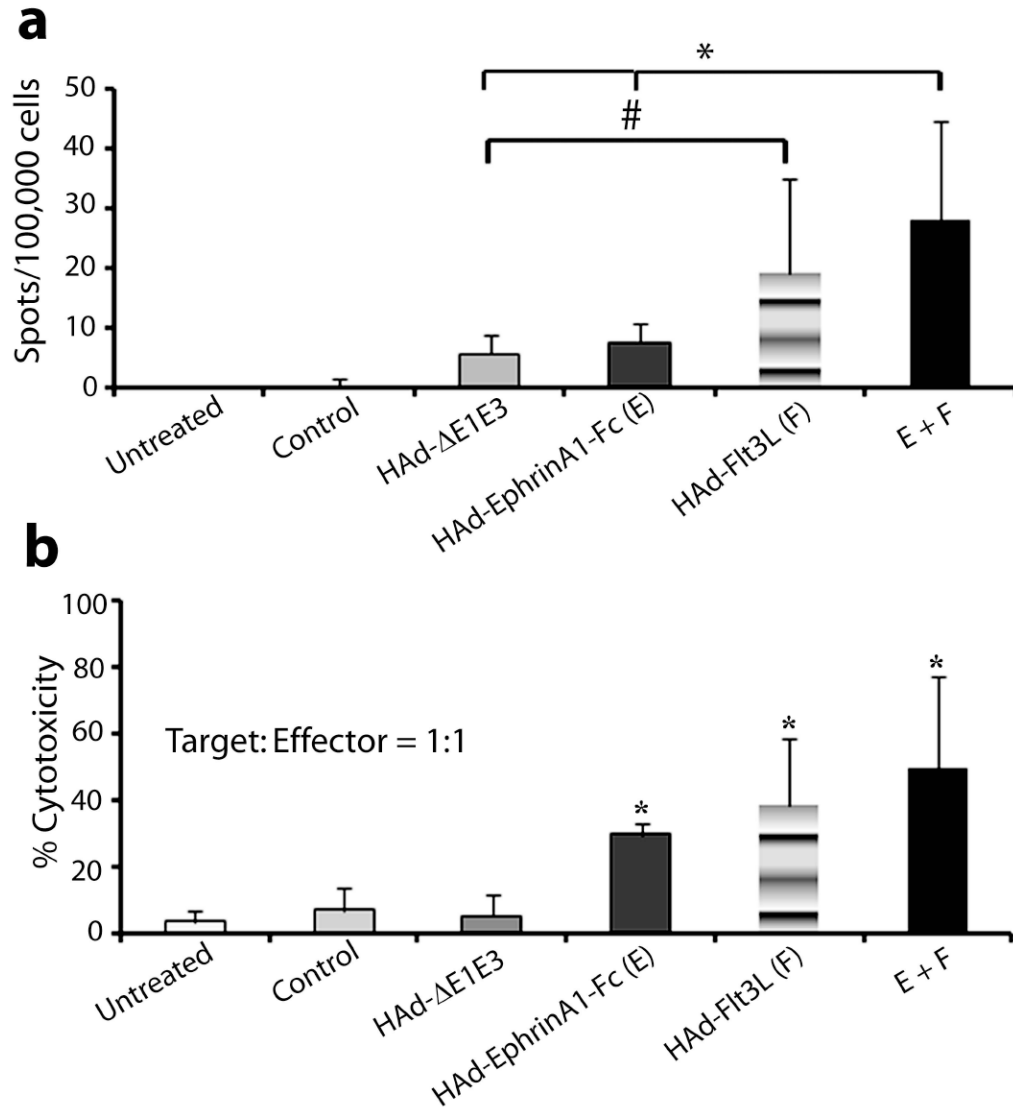


Figure 5. Induction of cell-mediated anti-tumor immune response in response to EphrinA1-Fc and Flt3L expression

(a) The tumor bearing mice were inoculated i.t. three times with PBS, HAd- E1E3, HAd-EphrinA1-Fc, HAd-Flt3L, or HAd-EphrinA1-Fc + HAd-Flt3L. Animals were euthanized at seven weeks post-inoculation, and the spleens were collected. Splenocytes were isolated and cultured in the presence of MT1A2 whole cell lysates. The number of IFN- γ secreting cells was monitored by ELISpot assay. (b) Splenocytes were co-cultured with mitomycin-treated MT1A2 cells for five days, and CD8+ T cells were purified by magnetic beads. The CD8+ T cells were co-cultured with MT1A2 cells in triplicate and assessed for cytotoxic activity by a colorimetric lactate dehydrogenase cytotoxicity assay. *, $P < 0.05$; #, $P < 0.1$ derived from unpaired t test.

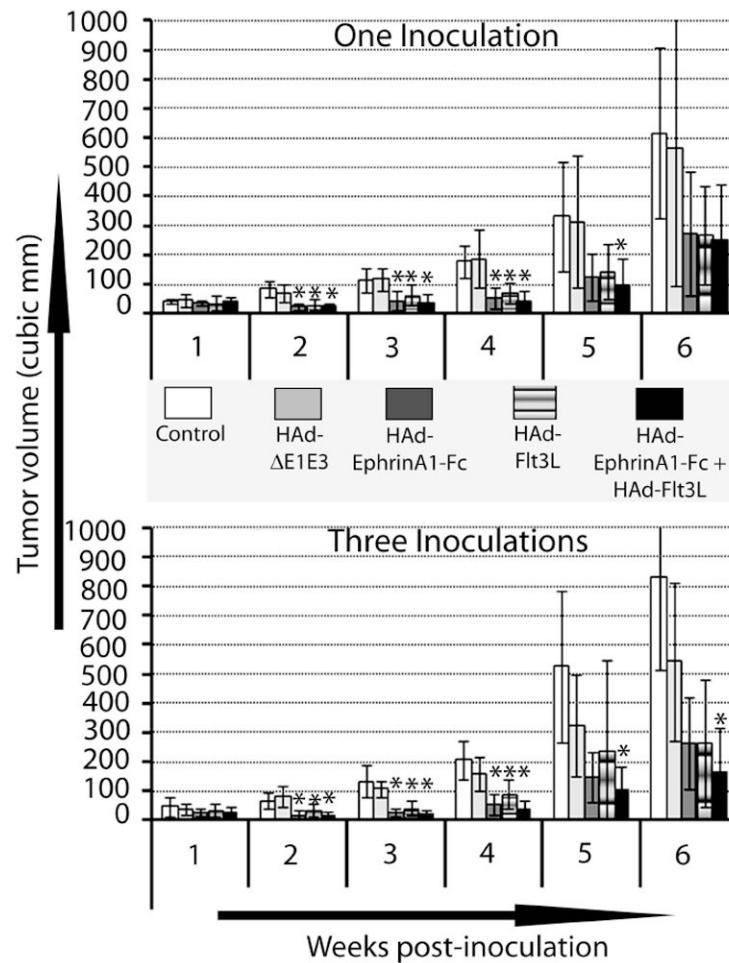


Figure 6. Inhibition in tumor growth in response to one or three i.t. inoculations of HAd-EphrinA1-Fc, HAd-Flt3L, HAd-EphrinA1-Fc + HAd-Flt3L in established tumors
Tumor-bearing mice were inoculated i.t. one or three times with PBS, HAd- E1E3, HAd-EphrinA1-Fc, HAd-Flt3L, or HAd-EphrinA1-Fc + HAd-Flt3L. The tumor growth was monitored by Vernier caliper measurements at a regular intervals, and the tumor volume was calculated by the formula $[\text{length} \times (\text{width})^2]/2$. *, $P < 0.05$ derived from ANOVA with Tukey's adjustments compared to empty vector (HAd- E1E3) control.